



## Synthesis and Characterization of Zinc Oxide Nanorods for Nitrogen Dioxide Gas Detection

Jong-Hyun Park, Hyojin Kim\*

Department of Materials Science and Engineering, Chungnam National University,  
Daejeon 34134, Republic of Korea

(Received 07 October, 2021 ; revised 17 October, 2021 ; accepted 26 October, 2021)

### Abstract

Synthesizing low-dimensional structures of oxide semiconductors is a promising approach to fabricate highly efficient gas sensors by means of possible enhancement in surface-to-volume ratios of their sensing materials. In this work, vertically aligned zinc oxide (ZnO) nanorods are successfully synthesized on a transparent glass substrate via seed-mediated hydrothermal synthesis method with the use of a ZnO nanoparticle seed layer, which is formed by thermally oxidizing a sputtered Zn metal film. Structural and optical characterization by x-ray diffraction (XRD), scanning electron microscopy (SEM), and Raman spectroscopy reveals the successful preparation of the ZnO nanorods array of the single hexagonal wurtzite crystalline phase. From gas sensing measurements for the nitrogen dioxide (NO<sub>2</sub>) gas, the vertically aligned ZnO nanorod array is observed to have a highly responsive sensitivity to NO<sub>2</sub> gas at relatively low concentrations and operating temperatures, especially showing a high maximum sensitivity to NO<sub>2</sub> at 250 °C and a low NO<sub>2</sub> detection limit of 5 ppm in dry air. These results along with a facile fabrication process demonstrate that the ZnO nanorods synthesized on a transparent glass substrate are very promising for low-cost and high-performance NO<sub>2</sub> gas sensors.

*Keywords : Zinc oxide, Oxide semiconductor, nanorod, NO<sub>2</sub> gas sensor, Hydrothermal synthesis*

## 1. Introduction

In the field of solid-state gas sensors, recent decades have seen an increasing interest in oxide semiconductor gas sensors due to their unique applications, including automotive and environmental applications [1]. The operating principle of these oxide semiconductor gas sensors is based on the phenomenon that the electrical resistivity of an oxide semiconductor varies with the composition and concentration

of the gas atmosphere surrounding it [2]. With a rapid development in thin film technology, oxide semiconductor thin films have become the most promising gas-sensing elements by virtue of their advantageous features, such as small dimensions, low cost, fabrication ease, and good compatibility with microelectronic processing [3]. However, there are still some limitations, especially relatively low sensitivity and high operating temperatures, in making practical gas sensors based on the oxide semiconductor thin films [4,5].

Among useful oxide semiconductors as gas sensing materials, zinc oxide (ZnO) has been intensively studied for the detection of toxic and

\*Corresponding Author: : Hyojin Kim  
Department of Materials Science and Engineering,  
Chungnam National University  
Tel: +82-42-821-6636 ; Fax: +82-42-822-5850 ;  
E-mail:hyojkim@cnu.ac.kr

inflammable gases such as  $H_2$ ,  $CO$ ,  $NH_3$ , and  $NO_2$ . Here our attention is focused on the detection of nitrogen dioxide ( $NO_2$ ), since the  $NO_2$  gas is one of the toxic atmospheric pollutants [6] and is commonly emitted from on-road vehicles, automobile industries, electricity generation and fossil fuel combustion [5]. To date, ZnO-based  $NO_2$  gas sensors with various forms of ZnO structures, including thin films, nanocrystalline ZnO and nanowires, have been demonstrated [7].

It is well recognized that the fabric of the microstructures of the sensing material ZnO has a distinct impact on the gas sensing performance of the ZnO-based gas sensors [8]. In this respect, recent advances in the synthesis of nanostructures with controllable size, shape, etc, provide a great opportunity for improving gas sensing properties [9]. Among them, one-dimensional (1D) ZnO nanostructures, such as nanowires, nanobelts, and nanorods, have attracted much attention by virtue of their great potential in gas sensing applications, not least due to their high surface-to-volume ratio. And various synthesis techniques of ZnO nanostructures, such as thermal evaporation, hydrothermal synthesis, sputtering, pulsed laser deposition, and molecular beam epitaxy, have been reported [10].

In the present paper, we report on the characterization of vertically aligned ZnO nanorods array synthesized on a transparent glass substrate via seed-mediated hydrothermal synthesis method with the use of a ZnO nanoparticle seed layer in order to serve as the sensing material for the  $NO_2$  gas detection. This work demonstrates a promising potential of the hydrothermally synthesized ZnO nanorods array as a gas-sensing element for an effective  $NO_2$  detection.

## 2. Experimental Details

The vertically-ordered ZnO nanorods array was prepared on a transparent glass substrate via a seed mediated hydrothermal technique with the use of a ZnO nanoparticle seed layer

formed via a two-step method [11]. To form the ZnO seed layer, Zn metal film was first deposited on the glass substrate from a pure Zn metal target. The Zn film was deposited under an Ar atmosphere of 5 mTorr for 3 min at room temperature (RT) by using a radio-frequency magnetron sputtering system with power of 20 W. Subsequently, the as-deposited Zn film was thermally oxidized in dry air at 400 °C for 1 h by using a rapid thermal annealing system to form ZnO nanoparticles, which acted as nucleation sites for ZnO nanorods. Aligned ZnO nanorods were prepared by dipping the ZnO-deposited substrate into a solution which consisted of 25 mM  $Zn(NO_3)_2 \cdot 6H_2O$  and 25 mM  $C_6H_{12}N_4$  in distilled water, and then heating it at 90 °C for 6 h in an oven. Finally, the substrate covered with ZnO nanorods was carefully cleaned with deionized (DI) water and dried under a high-purity nitrogen gas flow.

The crystalline phases of the prepared ZnO nanorods were characterized by X-ray diffraction (XRD) using  $K_\alpha$  radiation along with Raman spectroscopy, and then its microstructures were analyzed by scanning electron microscopy (SEM). The optical properties of the ZnO nanorods were examined by UV-vis-NIR spectrometer. The electrical and  $NO_2$  gas sensing properties of the ZnO nanorods were measured via two conductive electrodes by a multi-meter assembled in a computer-controlled gas sensing characterization system using flow-through method [8]. The fabricated gas sensing element was placed in a sealed chamber having one inlet and one outlet with electrical feedthrough. Carrier gas (dry air) and target gas ( $NO_2$ ) were loaded into the measurement chamber through the inlet port while the gases automatically came out through the outlet port due to the difference in pressure between the interior and exterior of the chamber. Before performing each measurement of gas sensing properties, the formation of an Ohmic contact between the ZnO active layer and electrodes was confirmed by the current-voltage

( $I$ - $V$ ) measurements, in which the applied voltage was varied from  $-3$  to  $+3$  V. For the gas sensing measurements, the applied dc voltage was fixed at  $2$  V and the change in current with time was recorded. The concentration of the target  $\text{NO}_2$  gas in dry air was controlled by adjusting the flow rate of the  $\text{NO}_2$  gas using separate mass flow controllers. The operating temperature was controlled using a small isolated hot plate integrated in the measurement chamber.

### 3. Results and Discussion

Typical scanning electron microscopy (SEM) images for the top-view and cross-sectional morphologies of the hydrothermally synthesized ZnO nanorods array on a glass substrate are shown in Figure 1(a) and 1(b), respectively. It is

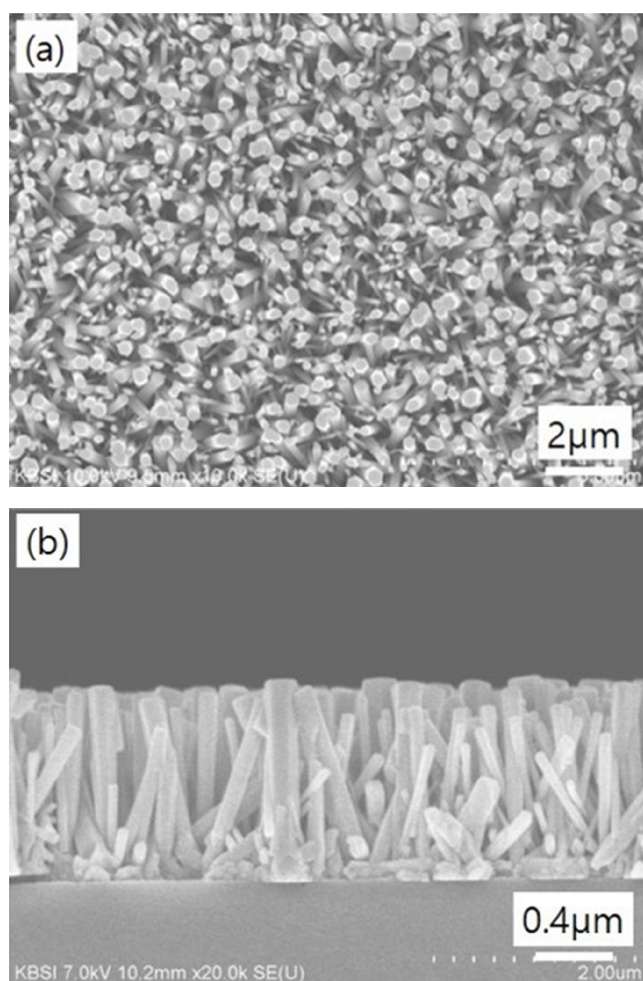


Fig. 1. Typical SEM images showing (a) top view and (b) cross-sectional view of the hydrothermally synthesized ZnO nanorods array on a glass substrate.

clearly seen from Figure 1(a) and 1(b) that the ZnO nanorods having a high degree of hexagonal orientation with an average diameter of  $\sim 80$  and an average length of  $\sim 2$  μm are vertically grown.

X-ray diffraction (XRD) was used to verify the formation of ZnO single crystalline phase. As presented in Figure 2(a), a typical XRD pattern of the synthesized ZnO nanorods array shows the diffraction peaks simply corresponding to the hexagonal wurtzite ZnO crystalline phase (JCPDS card. No. 36-1451) without any other second phases being detected, indicating the successful preparation of the ZnO nanorods of the single wurtzite phase.

The formation of the wurtzite ZnO crystalline phase can be further confirmed by the Raman spectroscopy analysis. Figure 2(b) shows the Raman spectrum of the hydrothermally synthesized ZnO

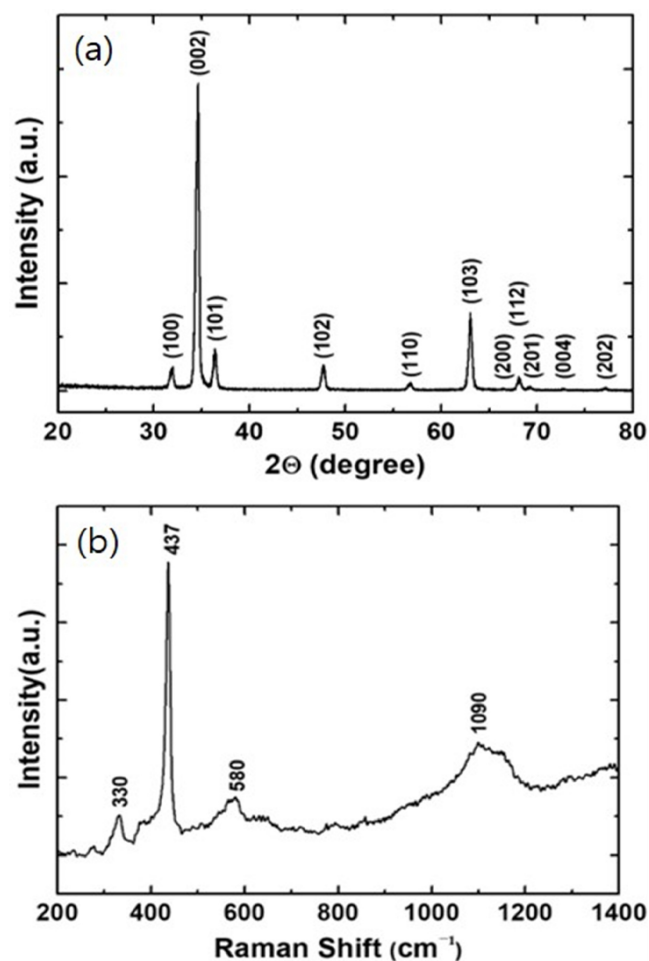


Fig. 2. (a) Typical X-ray diffraction pattern and (b) Raman spectrum of hydrothermally synthesized ZnO nanorods array on a glass substrate.

nanorods array on a glass substrate at room temperature. In these observed spectra, four distinct lines at 330, 437, 580, and 1090  $\text{cm}^{-1}$  correspond to the characteristic phonon frequencies of the wurtzite ZnO crystalline phase [12]. For the observed Raman lines from the ZnO phase, the lines at 330 and 437  $\text{cm}^{-1}$  are, respectively, assigned to the transverse optical phonon modes  $A_1$  (TO) and  $E_1$  (TO), the line at 580  $\text{cm}^{-1}$  is ascribed to the longitudinal phonon mode  $A_1$  (LO), and the line at 1090  $\text{cm}^{-1}$  comes from the acoustic combination of  $A_1$  and  $E_1$  phonon modes [12]. Consequently, both the observed XRD and Raman spectroscopy results further demonstrate the successful preparation of the ZnO nanorods of the single wurtzite phase.

Figure 3 shows the UV-vis-NIR absorbance spectrum of the hydrothermally synthesized ZnO nanorods array on a glass substrate at room temperature. It is clearly seen from Figure 3 that the ZnO nanorods array has an absorption edge at about 400 nm owing to the high band-gap energy of ZnO. In general, Tauc plot, which is obtained from the UV-vis-NIR spectrum, is used to determine the band-gap energy of semiconductor based on the following equation [13]:

$$(\alpha h\nu)^n = A(h\nu - E_g)$$

where  $\alpha$  is the absorption coefficient which can

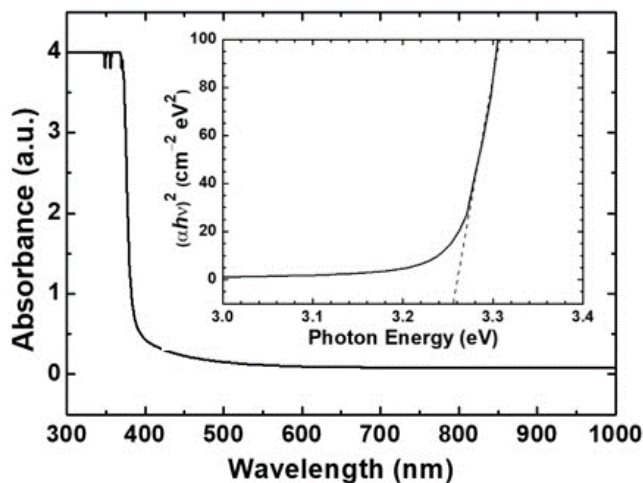


Fig. 3. Optical absorption spectrum of the hydrothermally synthesized ZnO nanorods on a glass substrate. The inset shows the Tauc plot for the prepared ZnO nanorods.

be obtained from UV-vis-NIR spectrum,  $h\nu$  is the energy of photon,  $A$  is a constant,  $E_g$  is the optical band-gap energy, and exponent  $n$  is dependent on the nature of the optical transition. It is known that  $n$  is 2 for direct transition and  $n$  is 1/2 for indirect transition [13]. As can be seen in the inset of Figure 3, a straight line is obtained when  $(\alpha h\nu)^2$  is plotted against photon energy ( $h\nu$ ), indicating that the absorption is owing to a direct transition for ZnO. The estimate band-gap energy of the hydrothermally synthesized ZnO nanorods array, which can be obtained from the intercept on the abscissa, is about 3.27 eV. This estimated value is found to be slightly smaller than the known standard value of 3.3 eV for the bulk ZnO [14].

The  $\text{NO}_2$  gas sensing properties of the ZnO nanorods array gas sensor were measured for various  $\text{NO}_2$  gas concentration and operating temperatures. The formation of an Ohmic contact between the ZnO nanorods array and electrodes was confirmed by observing a linear  $I$ - $V$  characteristic of the sensor, as shown in Figure 4(a). In Figure 4(b), we present the resistance response curves of the ZnO nanorods array gas sensor for a  $\text{NO}_2$  gas concentration of 10 ppm in dry air at various operating temperatures of 200, 225, 250, 275, and 300  $^{\circ}\text{C}$ . Here, the sensor response was calculated by the following relation defined as a ratio of the change in resistance upon exposure to the oxidizing  $\text{NO}_2$  target gas in dry air over the resistance in dry air,  $(R_g - R_a)/R_a$ , where  $R_a$  and  $R_g$  is the electrical resistance in dry air and upon exposure to the target gas in dry air, respectively. At each temperature, as can be seen in Figure 4(b), the resistance of the sensor increases somewhat abruptly when it is exposed to the oxidizing  $\text{NO}_2$  gas, exhibiting  $n$ -type semiconducting behavior upon exposure to an oxidizing gas as expected. It is clearly seen that the response characteristics of the sensor depend on the operating temperature. It is also found that the resistance measured after exposure to  $\text{NO}_2$  does not recover to the initial level. Such behavior can be explained by the presence of adsorbed gas molecules, which

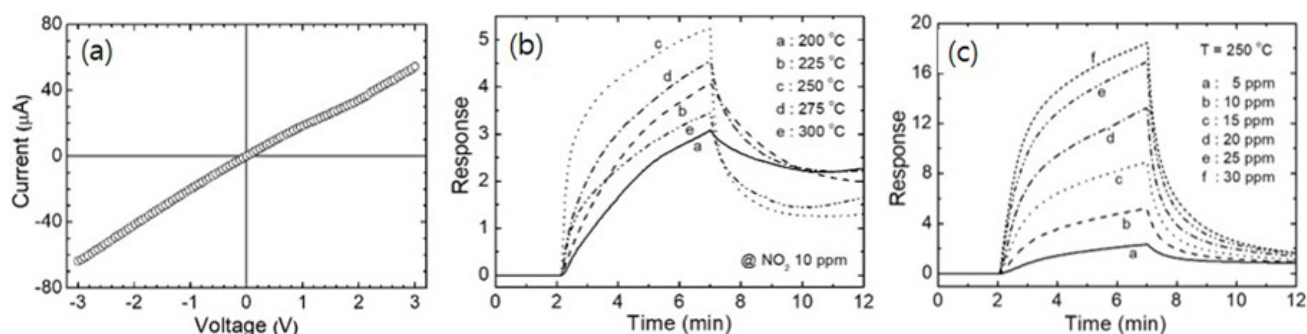
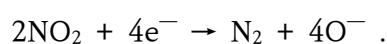


Fig. 4. (a) A representative  $I$ - $V$  characteristic curve of the ZnO nanorod gas sensor at room temperature. Typical transient response curves of the ZnO nanorod gas sensor (b) for a  $\text{NO}_2$  concentration of 10 ppm in dry air at various operating temperatures and (c) for several  $\text{NO}_2$  concentrations in dry air at the operating temperature of 250 °C.

were not removed from the surface of the ZnO nanorods. Furthermore, in Figure 4(c), we present the resistance response curves the ZnO nanorods array gas sensor operating at a temperature of 250 °C for various  $\text{NO}_2$  concentrations in dry air. The observed  $\text{NO}_2$  gas-sensing response evidently exhibits a distinct variation and increases with increasing  $\text{NO}_2$  concentration in dry air.

The gas sensing mechanism of the ZnO-based gas sensors for an oxidizing gas such as  $\text{NO}_2$  can be explained as follows. When a ZnO-based gas sensor is exposed to air, given that ZnO is intrinsically an  $n$ -type oxide semiconductor, oxygen from the ambient will adsorb on the exposed surface of ZnO and form an  $\text{O}_2^-$ ,  $\text{O}^-$  or  $\text{O}_2^-$  ion by capturing electrons from the ZnO conduction band [15,16]. Takata et al. revealed that the dominant adsorbed oxygen species in ZnO are  $\text{O}_2^-$ ,  $\text{O}^-$  and  $\text{O}_2^-$  for temperatures below 100 °C, between 100 and 300 °C, and above 300 °C, respectively [16]. When the sensor is exposed to an oxidizing gas, the gas will capture electrons from the ZnO conduction band and generate surface-adsorbed oxygen species, thus causing a change in the resistance of the sensor. In the range of 200 and 300 °C, the dominant surface interaction between ZnO and the oxidizing gas  $\text{NO}_2$  can be expressed as follows:



That is, by capturing electrons from the ZnO conduction band and decreasing the carrier

concentration in the ZnO active layer, the sensor's resistance is increased upon exposure to an oxidizing gas, as observed in Figures 4(b) and 4(c).

The sensitivity of the gas sensor is usually defined as the maximum response upon exposure to the target gas. Figure 5(a) shows the sensitivity of the ZnO nanorods array gas sensor as a function of the operating temperature upon exposure to 10-ppm  $\text{NO}_2$  in dry air. In general, the sensitivity of the gas sensor is affected by the operating temperature because of the strong influence of temperature on the adsorption-desorption of gases on the surface of the gas-sensing material. Figure 5(a) clearly illustrates that the sensitivity of the ZnO nanorods array gas sensor upon exposure to 10-ppm  $\text{NO}_2$  in dry air reaches a maximum value of 5.24, i.e. ~520% at an operating temperature of 250 °C, which is several times higher than that (~120%) of a nanostructured ZnO thin film  $\text{NO}_2$  gas sensor [5]. The observed enhancement in the sensitivity is most likely attributable to the higher surface-to-volume ratio associated with the vertically aligned ZnO nanorods and the resultant increase of the interaction strength between the target  $\text{NO}_2$  gas and the sensing ZnO layer.

Additionally, the variation of the sensitivity as a function of the  $\text{NO}_2$  concentration for the ZnO nanorods array gas sensor operating at the optimal temperature of 250 °C is shown in Fig. 5(b). The observed increase in the sensitivity  $S$  of the oxide semiconductor gas sensor with increasing target gas concentration can be empirically represented



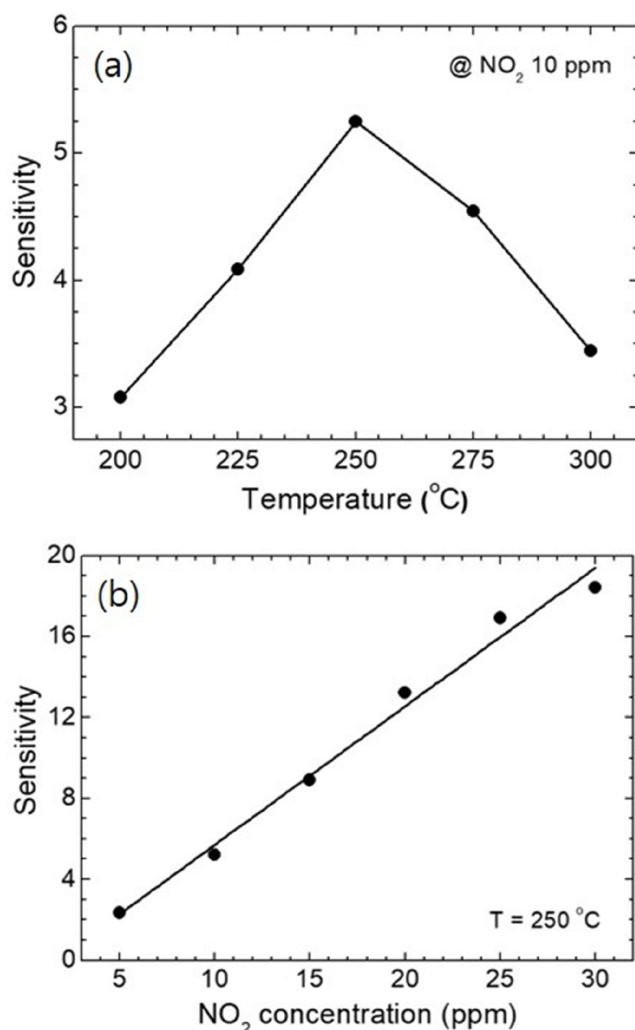


Fig. 5. (a) Sensor sensitivity versus operating temperature of the ZnO nanorod sensor when exposing to 10 ppm NO<sub>2</sub> in dry air. (b) Variation of the sensitivity as a function of NO<sub>2</sub> gas concentration for the ZnO nanorod sensor operated at 250 °C. The solid line is the fit curve of the empirical model,  $S \propto (P_g)^\beta$ .

as  $S = A(P_g)^\beta$ , where  $P_g$  is the partial pressure of the target gas, which is proportional to the gas concentration,  $A$  is a prefactor and  $\beta$  is an exponent [17]. In our case, the value of the exponent  $\beta$  is found to be about 1, as determined from the fitting curve shown as the solid line in Figure 5(b). Given that the ideal value of the exponent  $\beta$  is 1 for O<sup>-</sup> [17], the observed linear increase in the sensitivity with the NO<sub>2</sub> gas concentration at 250 °C indicates that the primary adsorbed oxygen species is O<sup>-</sup> as previously discussed by Takata et al. [16] for ZnO.

## 4. Conclusion

In summary, the vertically-oriented ZnO nanorods array to serve as the sensing material for the NO<sub>2</sub> gas detection have been successfully synthesized on a transparent glass substrate via seed-mediated hydrothermal synthesis method with the use of a ZnO nanoparticle seed layer, which is formed by thermally oxidizing a sputtered Zn metal film. The XRD, SEM, and Raman analyses reveal that the synthesized ZnO nanorods have a hexagonal wurtzite crystal structure with an average diameter of ~80 nm and an average length of ~2 μm. It is noted here that the sensitivity value of the ZnO nanorods array upon exposure to 10-ppm NO<sub>2</sub> gas was observed to be as high as ~520% at 250 °C, which is much greater than that of ZnO thin film NO<sub>2</sub> gas sensor. The observed better gas-sensing performance is ascribed to an enhancement in the area of possible surface reaction resulting from the vertically aligned nanorod structure. These results, along with the simple synthesis route, demonstrate the promising feasibility of fabricating low-cost, high-performance ZnO-based gas sensors.

## Acknowledgement

This research was supported by Basic Science Research Program through the National Research Foundation of Korea (NRF) funded by the Ministry of Education (NRF-2017R1D1A3B04030425).

## References

- [1] C.A. Grimes, E.C. Dickey, M.V. Pishko (Eds.), *Encyclopedia of Sensors*, American Scientific Publishers, Stevenson Ranch, 2006.
- [2] T. Seiyama, A. Kato, K. Fujishi, M. Nagatani, A new detector for gaseous components using semiconductive thin films, *Anal. Chem.* 34 (1962) 1502-1503.
- [3] G. Eranna, B.C. Joshi, D.P. Runthala, R.P.

- Gupta, Oxide materials for development of integrated gas sensors: a comprehensive review, *Crit. Rev. Solid State Mater. Sci.* 29 (2004) 111-188.
- [4] M. Aslam, V.A. Chaudhary, I.S. Mulla, S.R. Sainkar, A.B. Mandale, A.A. Belhekar, K. Vijayamohanan, A highly sensitive ammonia gas sensor using surface-ruthenated zinc oxide, *Sens. Actuators A* 75 (1999) 162-167.
- [5] V.L. Patil, S.A. Vanalakar, P.S. Patil, J.H. Kim, Fabrication of nanostructured ZnO thin films based NO<sub>2</sub> gas sensor via SILAR technique, *Sens. Actuators B* 239 (2017) 1185-1193.
- [6] U. Latza, S. Gerdes, X. Baur, Effects of nitrogen dioxide on human health: systematic review of experimental and epidemiological studies conducted between 2002 and 2006, *Int. J. Hyg. Environ. Health* 212 (2009) 271-287.
- [7] A. Afzal, N. Cioffi, L. Sabbatini, L. Torsi, NO<sub>x</sub> sensors based on semiconducting metal oxide nanostructures: progress and perspectives, *Sens. Actuators B* 171 (2012) 25-42.
- [8] N.L. Hung, H. Kim, S.-K. Hong, D. Kim, Enhancement of CO gas sensing properties in ZnO thin films deposited on self-assembled Au nanodots, *Sens. Actuators B* 151 (2010) 127-132.
- [9] N.L. Hung, H. Kim, S.-K. Hong, D. Kim, A simple fabrication method of randomly oriented polycrystalline zinc oxide nanowires and their application to gas sensing, *Adv. Nat. Sci.: Nanosci. Nanotechnol.* 2 (2011) 015002 (6pp).
- [10] Y. Xia, P. Yang, Y. Sun, Y. Wu, B. Mayers, B. Gates, Y. Yin, F. Kim, H. Yan, One-dimensional nanostructures: synthesis, characterization, and applications, *Adv. Mater.* 15 (2003) 353-389.
- [11] J.-H. Park, H. Kim, Photoelectrochemical properties of a vertically aligned zinc oxide nanorod photoelectrode, *J. Korean Inst. Surf. Eng.* 51 (2018), 237-242.
- [12] R. Zhang, P.-G. Yin, N. Wang, L. Guo, Photoluminescence and Raman Scattering of ZnO nanorods, *Solid State Sci.* 11 (2009) 865-869.
- [13] P. Sinsermsuksakui, J. Heo, W. Noh, A.S. Hock, R.G. Gordon, Atomic layer deposition of tin monosulfide thin films, *Adv. Energy Mater.* 1 (2011) 1116-1125.
- [14] V. Srikant, D.R. Clarke, On the optical band gap of zinc oxide, *J. Appl. Phys.* 83 (1998) 5447-5451.
- [15] M. Che, A.J. Tench, Characterization and reactivity of mononuclear oxygen species on oxide surfaces, *Adv. Catal.* 31 (1982) 77-133.
- [16] M. Takata, D. Tsubone, H. Yanagida, Dependence of electrical conductivity of ZnO on degree of sintering, *J. Am. Ceram. Soc.* 59 (1976) 4-8.
- [17] R.W.J. Scott, S.M. Yang, G. Chabanis, N. Coombs, D.E. Williams, G.A. Ozin, Tin dioxide opals and inverted opals: near-ideal microstructures for gas sensor, *Adv. Mater.* 13 (2001) 1468-1472.